A Comparison of Surface Simplification Strategies for Realistic Grains

Danilo Menezes Santos[1], Alfredo Gay Neto[1]

[1]*Dept. of Structural and Geotechnical Engineering, Polytechnic School at University of São Paulo*
Av. Prof. Luciano Gualberto, 380 - Butantã, 05508-010, São Paulo, Brazil
dmsantosse@usp.br, alfredo.gay@usp.br

Abstract. In recent years, the Discrete Element Method (DEM) has emerged as a powerful tool for studying granular materials. In a DEM simulation, the aim is to reproduce grain-to-grain interactions, providing new insights into the overall mechanical behavior of the granular system. From the earliest stages of DEM, particles were represented by disks or spheres. Currently, many codes have been developed to incorporate new ways of representing the grain shape more accurately. However, this process is not simple, as more realistic shapes require more complex algorithms for contact detection, which can even make simulations unfeasible in some cases. In the case of polyhedra, an alternative to circumvent this problem is to reduce the number of entities in the mesh, reducing the computational cost of the simulation and the level of fidelity to the real shape of the grain. Understanding that this preprocessing stage is fundamental to DEM, this article compares the impact in shape descriptors of 30 particles, when three different strategies for mesh simplification are employed.

Keywords: Discrete Element Method; Realistic Grains; Shape Descriptors

1 Introduction

For a long time, assumptions about the behavior of granular systems were based on visualizing experimental tests and using intuition (Thorton [1]). In recent years, the study of these materials has been improved by the incorporation of imaging tools such as X-ray tomography (Matsumura et al [2]) and Scanners (Tang et al [3]), which have enabled the investigation of these systems from a microscopic viewpoint.

Through this advance, it has been observed that several macroscopic behaviors in granular media are correlated with the morphology and size of the particles in their composition. For example, according to Babak and Resnik [4], the particle size distribution influences the permeability index of the sands. In the same way, the segregation of materials, as seen in the Brazilian nut phenomena, is affected by the size of the grains present in the mixture (Mobius et al. [5]). Moreover, a range of morphological indices, including sphericity, volume, surface area, convexity, and aspect ratio, are of crucial importance in determining the thermal shear resistance, void ratio, and other mechanical properties of soil (Cho, Dodds and Santamarina [6]).

At the same time, as highlighted by Thorton [1], the increase in computing power has allowed the behavior of granular materials to be simulated using numerical methods. In this context, the Discrete Element Method (DEM), originally proposed by Cundall and Strack [7], has become a relevant tool for the analysis of granular media, such as soils, powders, and ballast. The DEM is formulated as a discontinuous method, where the particles present in a granular medium are represented in the simulation by numerical entities that can move freely and interact with each other, according to Newton's Laws (O'Sullivan [8]). This explicit discretization of particles represents one of the main advantages of the method. Due to that, the influence of rotations, translations, and particle contacts on the macroscopic behavior of the system can be quantified (Thorton [1]).

In several implementations of DEM, spheres are employed to represent the real grain shape (Ferellec and McDowell [9]). The adoption of spherical objects allows contact detection and force calculation to depend solely on the contact normals and relative displacements from the branch vector and the radii of the contact elements (Duriez and Bonelli [10]). In this manner, less computation is required, and systems with large numbers of particles can be analyzed (O'Sullivan [8]).

However, in the situation when the granular medium consists of grains with sharp edges and concavities, such as ballast and tailings, the utilization of spheres may be a coarse approximation. According to Ferellec and McDowell [9], this type of difference between the real and numerical shape of the particles can limit the DEM's ability to reproduce the quantitative behavior of the system under study.

To avoid these limitations, new formulations of the method have been developed using shapes closer to real particles, such as ellipses, superquadrics, NURBS, clusters, polyhedra, and others. In general, the adoption of these shapes makes the DEM workflow more complex, requiring more robust algorithms that significantly increase the computational time required to perform the simulation (Neto and Wriggers [11]).

An alternative found by DEM users, for some particle modeling choices, such as polyhedra, is to perform a preprocessing step reducing the number of faces, edges, and vertices used to describe the real grain to decrease the computational problems (Guo et al. [12]). By modifying the particle geometry, this simplification process must be done carefully so that the main characteristics of the particles are not lost (Feng [13]). Understanding the necessity of this balance between shape representation and computational resources, in this paper, three different strategies are used to reduce the number of entities of 30 realistic particles, and the capacity of each algorithm to maintain the geometric representation of grains is quantified by a set of shape descriptors important in simulations employing DEM.

2 Methodology

In our study, 30 realistic grains used by Santos and Neto [14] were randomly chosen. These particles are mathematically described by Spherical Harmonics Functions (SPH) and through this parameterization, the positions x, y, and z of any i point in particle perimeter are defined by an azimuth (ϕ) and elevation angle (θ), according to eq. (1):

$$x_i = \sum_{n=0}^{\infty} \sum_{m=-n}^{n} c_{x_n}^{m} Y_n^m(\phi, \theta), |y_i = \sum_{n=0}^{\infty} \sum_{m=-n}^{n} c_{y_n}^{m} Y_n^m(\phi, \theta), |z_i = \sum_{n=0}^{\infty} \sum_{m=-n}^{n} c_{z_n}^{m} Y_n^m(\phi, \theta), \qquad (1)$$

where the variables n and m are associated with Legendre Function, the $c_{x_n}^{m}$, $c_{y_n}^{m}$, $c_{z_n}^{m}$ are the spherical harmonics coefficients to degree n and order m, and $Y_n^m(\phi, \theta)$ the spherical harmonic at degree n. Using different combinations of ϕ and θ a total of 10000 points were created on the surface of each particle, in sequence a triangulation algorithm was applied and the 30 polyhedron particles shown in Figure 1 were generated. The surface of each grain is composed of 20000 triangles, which is a sufficient number to represent the SPH particle surface as observed in previous works of Zhao et al [15] and Zhu et al [16].
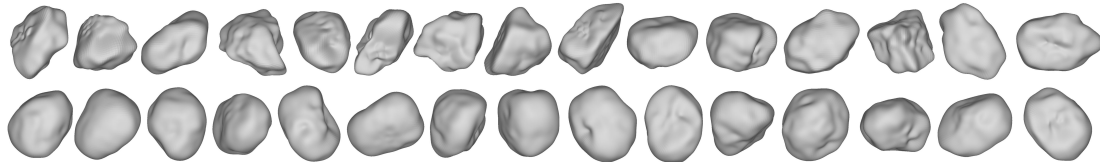

Figure 1. Polyhedron representation of the grains. In the first row are located the particles: A2, A8, A9, A16, A26, A33, A44, A49, A56, A73, A82, A96, A101, A105, and A108. In the second row are located the particles: O1, O18, O26, O27, O33, O45, O57, O68, O74, O89, O92, O100, O107, O114, and O121.

To perform our experiment, the Quadric Edge Error developed by Garland and Hackbert [17] was the first simplification approach used. This algorithm is a general method for reducing entities in triangular meshes of surfaces, with a wide range of applications in computer graphics. In its operation, successive iterations are performed to identify the pair of vertices that, when merged, will result in the least geometric error between the current and the next iteration mesh. In this study, the implementation present in the Meshlab software [18] was used, through which a set of 13 different properties can be defined to achieve a simplified particle with the number of faces desired. Due to the lack of physical interpretation of some of their properties, only the target number of faces and the "preserve topology" checkbox were set differently from the default in the software.

In contrast to the first approach, which is a general method, the second and third strategies can be applied only to grains parametrized through Spherical Harmonic Functions. Although these methods are somewhat restrictive, the objective is to transform the reconstruction and simplification stages of the polyhedral particle into a single one. It is possible to directly determine the parametric coordinates, specifically ϕ and θ, which recreate the polyhedron with the desired number of triangles and shape descriptors closest to those in Figure 1.

From this assumption, the second scheme divides the rectangular parametric domain into equal divisions along both, the ϕ and θ, directions as shown in Figure 2a. From this division, the parametric space is triangularized

to split each square into two triangles. Utilizing the parametric coordinates from each point in parametric space in eq. (1), the surface of the SPH particle is created, and the triangles' connectivity is the one of the parametric space. This is a commonly used technique to generate polyhedra from Spherical Harmonics Functions in DEM context [13], and the number of entities in the mesh can be directly controlled by the number of divisions of the parametric space.
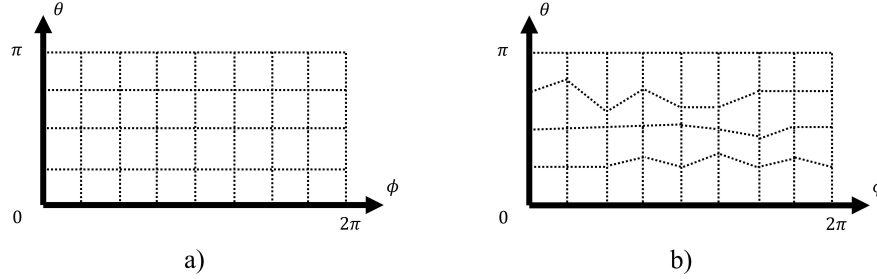

a)   b)

Figure 2. Parametric space division.

According to Feng [13], despite its simplicity, this process of triangularization presents severe distortion near the two poles of a particle, where too many vertices are located. To circumvent this problem, the third simplification scheme applies an optimization algorithm to modify the coordinates θ of the squares, with the objective that the points on the SPH surface that share the same value of ϕ are equidistant. Figure 2b presents an example of parametric space representation for this situation, and Table 1 shows the optimization problem formulated.

Algorithm 1 Optimization Problem

$N \leftarrow$ number of subdivision
$\Delta = \frac{2\pi}{N}$
for $j = 0, 1, 2, \ldots, N$ **do**
    $\phi = j * \Delta$
    minimize $f(\theta_1, \theta_2, \theta_3, \ldots, \theta_{N-1})$
    subject to:
    $f(\theta_1, \theta_2, \theta_3, \ldots, \theta_{N-1}) = \sum_{i=1}^{i=N-1}(L_{i-1} - L_i)^2$
    $\theta_0 = 0$
    $\theta_N = \pi$
    $L_i = \sqrt{(x(\phi_i, \theta_i) - x(\phi_{i+1}, \theta_{i+1}))^2 + (y(\phi_i, \theta_i) - y(\phi_{i+1}, \theta_{i+1}))^2 + (z(\phi_i, \theta_i) - z(\phi_{i+1}, \theta_{i+1}))^2}$
    $-\theta_i + \theta_{i+1} \leq 1/1000$
end for

By employing the three strategies, polyhedra with 18, 98, and 200 triangular faces were generated. To simplify the particles in Meshlab, only the target number of faces and the "preserve topology" checkbox were set differently from the default. In the second and third methods, the same number of divisions were used in the axis ϕ and θ. In the comparison shown in chapter 3, the simplified grains have the volume (Vol), surface area (S), sphericity, convexity (Cx), and aspect ratio (AC and BC) computed, and compared to the values of target particles of Figure 1.

3 Results

Figure 3 shows a visual perspective of simplified particles with 200 triangles produced by the three methods. In general, the three sets of simplified particles maintain the main characteristics of target particles, with the Meshlab particles having a better representation of the concavities of the particles.

In addition, Figure 4 shows the results obtained when only 18 faces are used. In this case, the particles simplified by "method 2" and "method 3" become very different from the target particles, while the use of Meshlab was able to reproduce the expected result more accurately. It is interesting to note that, due to the small number of triangles used, there is a notable reduction in the number of concavities present in the particle.

To complement the visual analysis, some shape descriptors that potentially may have a significant impact on the numerical simulations of DEM simulations were calculated and compared to those of the target particles. Figure 5 shows the results for Volume and Surface Area, and as can be seen in the case of the three simplification methods, as the number of faces is increased the shape descriptor is closer to the target values. Furthermore,

through the Meshlab algorithm, even with a few triangles, around 75% of the shape descriptor of the real particle can be recovered. Figure 6 shows the values for sphericity and concavity. The use of Meshlab again proved to be
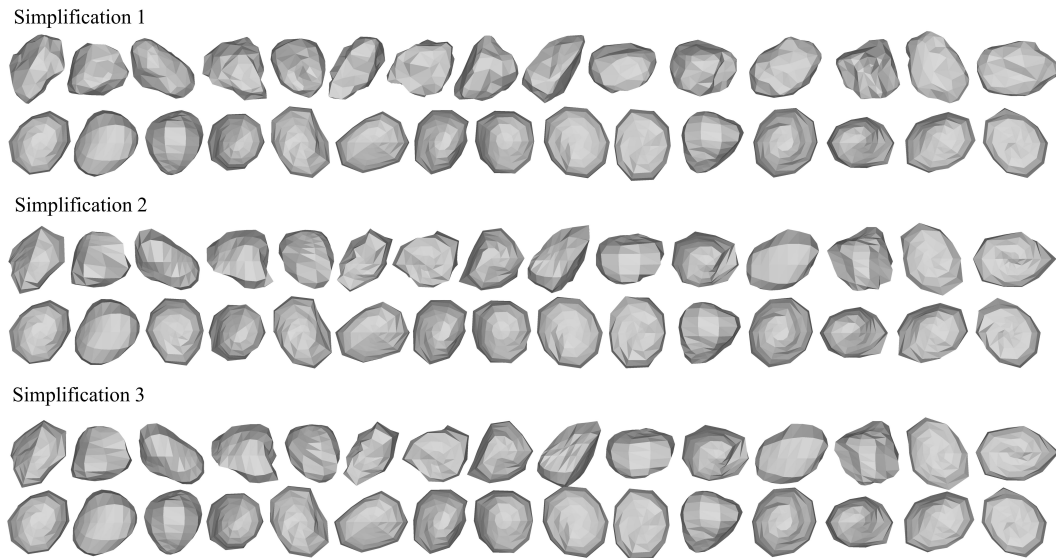
Simplification 1

Simplification 2

Simplification 3

Figure 3. Simplified particles with 200 triangular faces.

Simplification 1

Simplification 2

Simplification 3
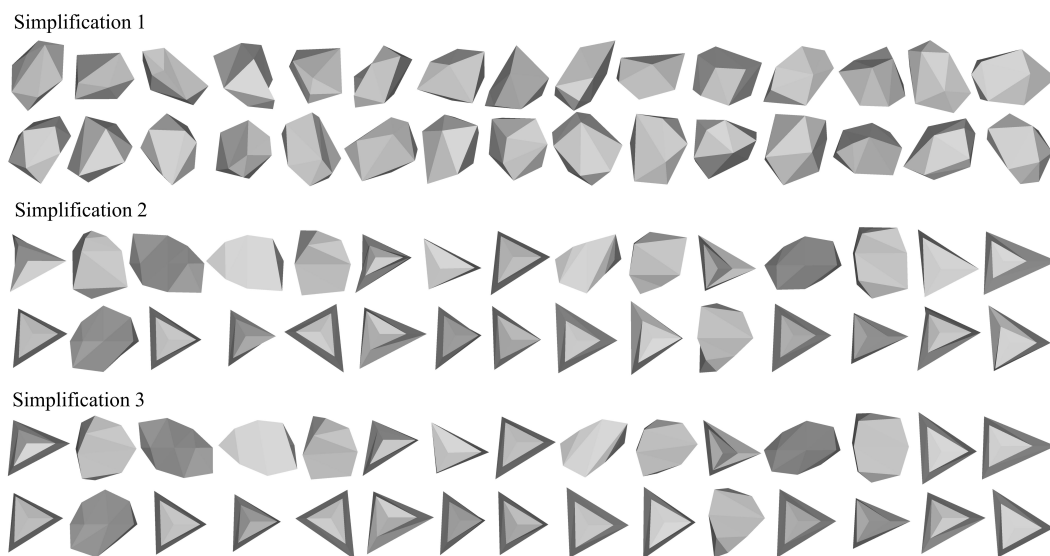
Figure 4. Simplified particles with 18 triangular faces.

better, with more particles having their properties close to the expected value. However, it should be noted that for grains where a rounder shape is seen, the use of the optimization algorithm was better.

In the end, the ratio between the dimensions of the oriented bounding box was analyzed. In Figure 7, C represents the largest measurement of the particle, A is the second largest measurement, and B is the smallest measurement of the particle. In the results analyzed here, a greater variation of aspect ratio can be observed in the coarse mesh, and the increase of triangles number provides a reduction of the overall error.

4 Conclusions

The analysis showed that Quadric Edge Error provided the best results for producing simplified polyhedral particles.

It can also be seen that little difference was observed in the shape descriptors of the particles simplified by other two methods, which indicates that the distortions in the poles obtained by "method 2" had little influence on

the analysis of these parameters.

It should be noted that the conclusions reached here only deal with the characteristics of the particles. It is suggested that future analyses be complemented by analyzing the impact that the simplified particles would have on the numerical simulations, or by investigating other characteristics of the particles.
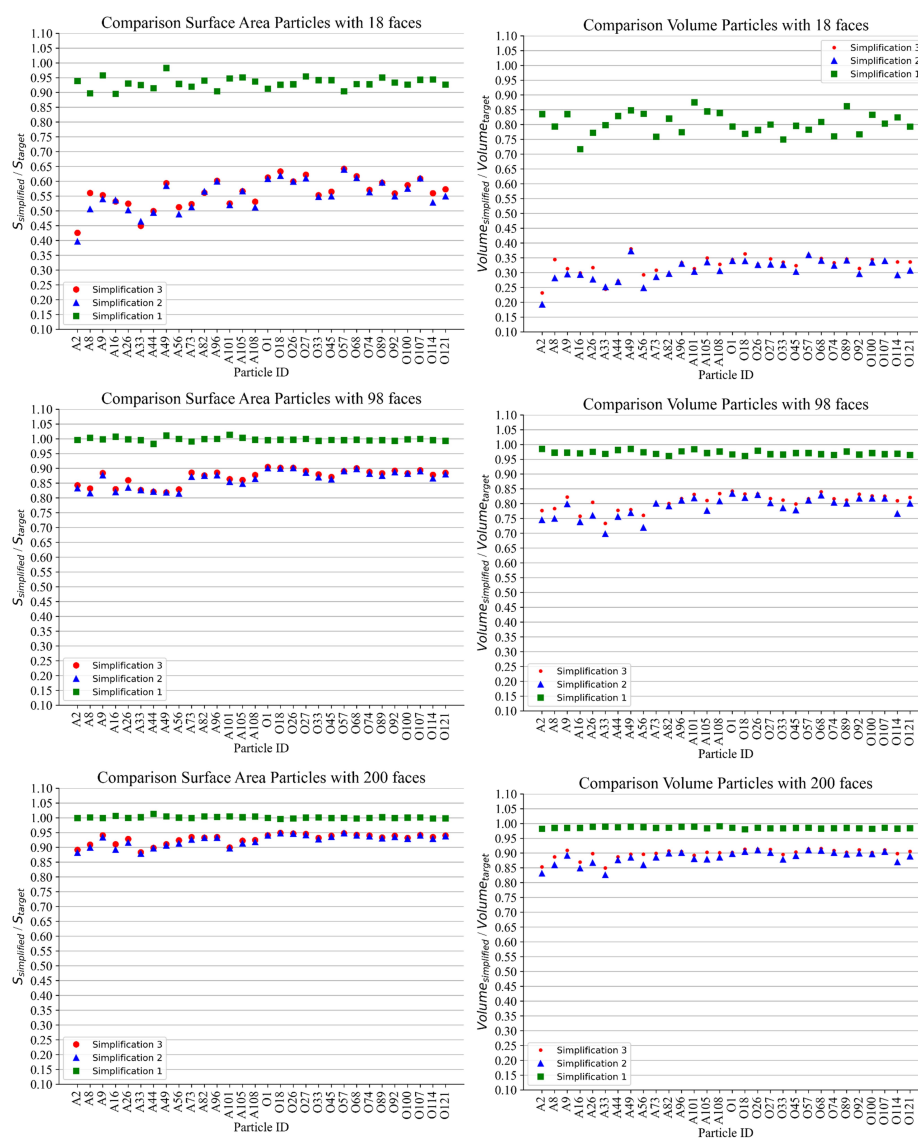

Figure 5. Comparison between Volume and Surface Area of simplified and target particles.

Authorship statement. The authors hereby confirm that they are the sole liable persons responsible for the authorship of this work, and that all material that has been herein included as part of the present paper is either the property (and authorship) of the authors, or has the permission of the owners to be included here.

References

[1] C. Thornton. *Granular Dynamics, Contact Mechanics and Particle System Simulations: A DEM study*, volume 24 of *Particle Technology Series*. Springer International Publishing, Cham, 2015.

Figure 6. Comparison between Convexity and Sphericity of simplified and target particles.

[2] S. Matsumura, A. Kondo, K. Nakamura, T. Mizutani, E. Kohama, K. Wada, T. Kobayashi, N. Roy, and J. D. Frost. 3D image scanning of gravel soil using in-situ X-ray computed tomography. *Scientific Reports*, vol. 13, n. 1, pp. 20007, 2023.

[3] C.-S. Tang, Q. Cheng, X. Gong, B. Shi, and H. I. Inyang. Investigation on microstructure evolution of clayey soils: A review focusing on wetting/drying process. *Journal of Rock Mechanics and Geotechnical Engineering*, vol. 15, n. 1, pp. 269–284, 2023.

[4] O. Babak and J. Resnick. On the Use of Particle Size Distribution Data for Permeability Modeling. In *Day 2 Wed, June 11, 2014*, pp. D021S005R005, Calgary, Alberta, Canada. SPE, 2014.

[5] M. E. Möbius, B. E. Lauderdale, S. R. Nagel, and H. M. Jaeger. Size separation of granular particles. *Nature*, vol. 414, n. 6861, pp. 270–270, 2001.

[6] G.-C. Cho, J. Dodds, and J. C. Santamarina. Particle Shape Effects on Packing Density, Stiffness, and Strength: Natural and Crushed Sands. *Journal of Geotechnical and Geoenvironmental Engineering*, vol. 132, n. 5, pp. 591–602, 2006.

[7] P. A. Cundall and O. D. L. Strack. A discrete numerical model for granular assemblies. *Géotechnique*, vol. 29, n. 1, pp. 47–65, 1979.

[8] C. O'Sullivan. *Particulate discrete element modelling: a geomechanics perspective*, 2011.

[9] J.-F. Ferellec and G. R. McDowell. A method to model realistic particle shape and inertia in DEM. *Granular Matter*, vol. 12, n. 5, pp. 459–467, 2010.

[10] J. Duriez and S. Bonelli. Precision and computational costs of Level Set-Discrete Element Method (LS-DEM) with respect to DEM. *Computers and Geotechnics*, vol. 134, pp. 104033, 2021.
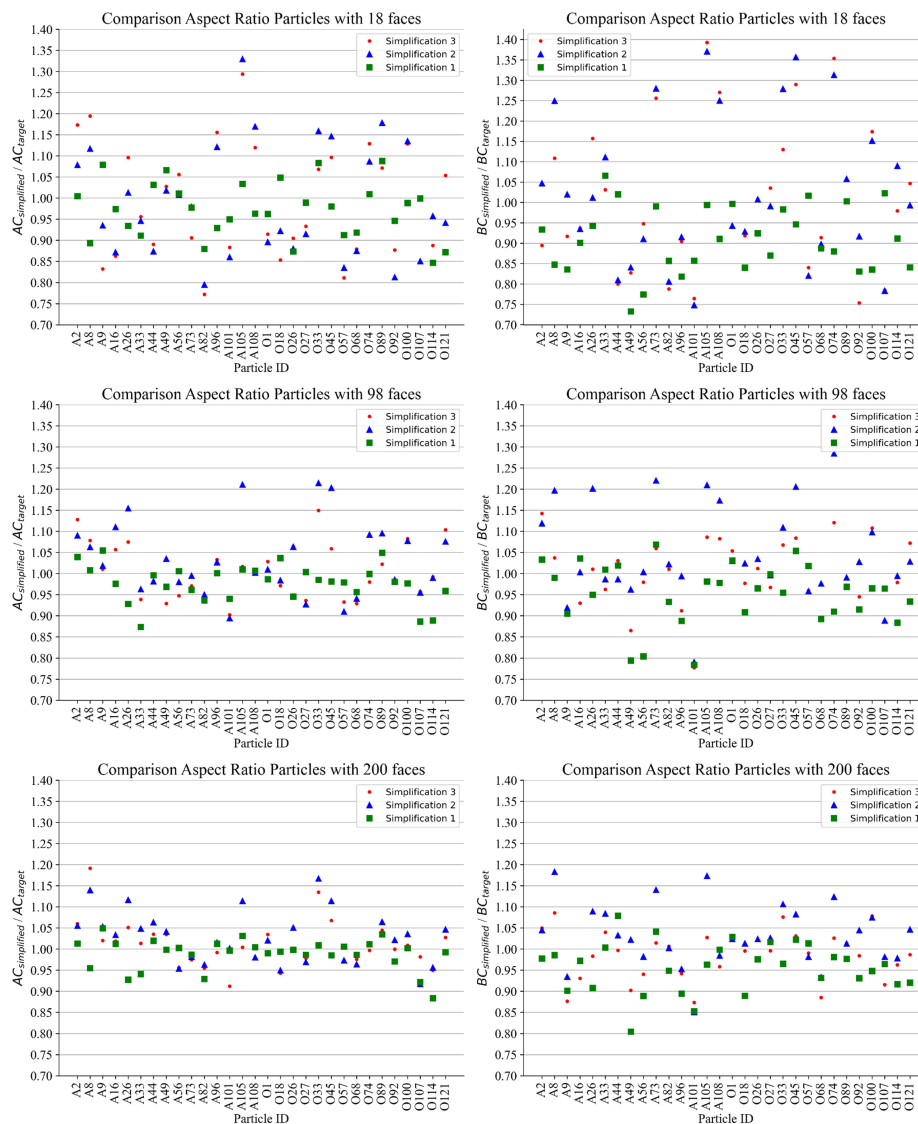
CILAMCE-2024

Proceedings of the XLV Ibero-Latin-American Congress on Computational Methods in Engineering, ABMEC
Maceió, Alagoas, November 11-14, 2024

Figure 7. Comparison between the Aspect Ratio of simplified and target particles.

[11] A. G. Neto and P. Wriggers. Discrete element model for general polyhedra. *Computational Particle Mechanics*, vol. 9, n. 2, pp. 353–380, 2022.

[12] Y. Guo, C. Zhao, V. Markine, G. Jing, and W. Zhai. Calibration for discrete element modelling of railway ballast: A review. *Transportation Geotechnics*, vol. 23, pp. 100341, 2020.

[13] Y. Feng. An effective energy-conserving contact modelling strategy for spherical harmonic particles represented by surface triangular meshes with automatic simplification. *Computer Methods in Applied Mechanics and Engineering*, vol. 379, pp. 113750, 2021.

[14] D. M. Santos and A. G. Neto. Considerations on the ability of supervised neural networks to infer the 3d shape of particles from 2d projections, (Manuscript submitted for publication).

[15] B. Zhao, D. Wei, and J. Wang. Particle shape quantification using rotation-invariant spherical harmonic analysis. *Géotechnique Letters*, vol. 7, n. 2, pp. 190–196, 2017.

[16] Z. Zhu, H. Chen, W. Xu, and L. Liu. Parking simulation of three-dimensional multi-sized star-shaped particles. *Modelling and Simulation in Materials Science and Engineering*, vol. 22, n. 3, pp. 035008, 2014.

[17] M. Garland and P. S. Heckbert. Surface simplification using quadric error metrics. In *Proceedings of the 24th annual conference on Computer graphics and interactive techniques*, pp. 209–216, 1997.

[18] P. Cignoni, M. Callieri, M. Corsini, M. Dellepiane, F. Ganovelli, and G. Ranzuglia. MeshLab: an Open-Source Mesh Processing Tool. In V. Scarano, R. D. Chiara, and U. Erra, eds, *Eurographics Italian Chapter Conference*. The Eurographics Association, 2008.